Biochimica et Biophysica Acta 1827 (2013) 1020–1030

Contents lists available at SciVerse ScienceDirect

Biochimica et Biophysica Acta

journal homepage: www.elsevier.com/locate/bbabio

Review

Reflections on substrate water and dioxygen formation ☆,☆☆

Nicholas Cox [a], Johannes Messinger [b,*]

[a] Max-Planck-Institut für Chemische Energiekonversion, Stiftstrasse 34-36, D-45470 Mülheim an der Ruhr, Germany
[b] Department of Chemistry, Chemistry Biology Centre (KBC), Umeå University, Linnaeus väg 6, S-90187 Umeå, Sweden

ARTICLE INFO

Article history:
Received 14 December 2012
Received in revised form 23 January 2013
Accepted 25 January 2013
Available online 1 February 2013

Keywords:
Photosystem II
Substrate water binding
Mechanism of water oxidation
Water oxidizing complex (WOC)
Oxygen evolving complex (OEC)
Mn_4CaO_5 cluster

ABSTRACT

This brief article aims at presenting a concise summary of all experimental findings regarding substrate water-binding to the Mn_4CaO_5 cluster in photosystem II. Mass spectrometric and spectroscopic results are interpreted in light of recent structural information of the water oxidizing complex obtained by X-ray crystallography, spectroscopy and theoretical modeling. Within this framework current proposals for the mechanism of photosynthetic water-oxidation are evaluated. This article is part of a Special Issue entitled: Metals in Bioenergetics and Biomimetics Systems.

1. Introduction

The light-driven water–plastoquinone oxidoreductase photosystem II (PSII) catalyzes the reaction:

$$2H_2O + 2PQ + 4^{+}_{stroma} \xrightarrow{4h\nu(440-680\ nm)} O_2 + 2PQH_2 + 4H^{+}_{lumen}. \quad (1)$$

Reaction (1) is energetically uphill. It is driven by four light-induced charge separations in the reaction center of PSII, a multipigment assembly of four chlorophylls and two pheophytins. A cascade of fast electron transfer reactions stabilizes the initial charge separation by increasing the distance between the 'hole' and the electron, which as a consequence reduces the energy difference between the acceptor/donor pair, i.e. the driving force for charge recombination. These 'wasteful' secondary electron transfer processes extend the lifetime of the charge separated state such that the complex multi-electron and multi-proton chemistry of plastoquinone reduction and water oxidation can take place with greater than 90% quantum efficiency under optimal light conditions. Minimizing back reactions also reduces harmful singlet oxygen formation and thereby increases the long term stability of PSII [1]. In addition to accumulating reducing equivalents (in the form of plastoquinol) PSII also contributes significantly to the buildup of a proton gradient across the thylakoid membrane that is employed by the ATPase for the conversion of ADP to ATP.

The overall structure of PSII and the sequence of electron transfer events constituting its primary function are already well understood and are described in detail in many original papers and review articles (see e.g. [2–11]). As such, this short account is limited to only one aspect of research on PSII, substrate water binding to the water-oxidizing complex (WOC). This functional unit harbors the water-splitting cluster, an inorganic Mn_4CaO_5 complex, which is ligated by one histidine, six carboxylate ligands, and four water-derived terminal ligands (W1–W4 in Fig. 1). The WOC also comprises second sphere waters that form a H-bonding network around the cluster extending up to tyrosine Y_Z (D1-Y161) and histidine 190 of the D1 protein (D1-H190). These structural waters are positioned by second sphere amino acids of which some form H-bonds to oxo-bridges or water ligands of the cluster, for example D1-H337, CP43-R357 and D1-D61 [8–10] (Fig. 1). The main function of the WOC is to couple the *ps* one-electron photochemical charge separations of the chlorophyll/pheophytin reaction center with the four-electron, four-proton chemistry of water-oxidation to molecular oxygen, which occurs in the *ms* time domain. To do so, the WOC undergoes a cycle of five oxidation states known as S_0, S_1, S_2, S_3 and S_4 states (Kok cycle; Fig. 2) [12,13], where the index refers to the number of stored oxidizing equivalents. Since the WOC is always oxidized by $Y_Z^{\bullet}$, the redox potential steps between the different S_i states must be similar. This requires a strictly alternating sequence of electron and proton removals from the WOC

☆ This article is part of a Special Issue entitled: Metals in Bioenergetics and Biomimetics Systems.

☆☆ JM dedicates this review to the memory of Gernot Renger (October 23, 1937–January 12, 2013), who was his PhD supervisor, mentor, collaborator and friend. With his excellent knowledge of the literature that covered almost all aspects of photosystem II, and through his detailed, independent and systematic thinking Gernot Renger made outstanding contributions to the understanding of the functioning of photosystem II and of water-splitting in particular.

* Corresponding author. Tel.: +46 907865933.
E-mail address: Johannes.Messinger@chem.umu.se (J. Messinger).

0005-2728
http://dx.doi.org/10.1016/j.bbabio.2013.01.013

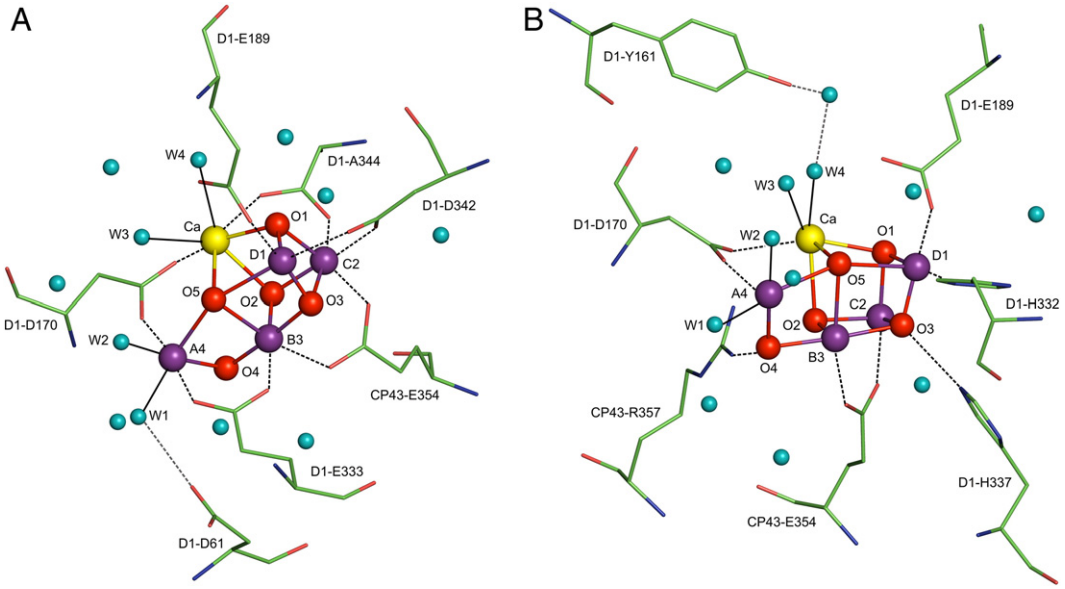

Fig. 1. Structure of the water-oxidizing complex based on X-ray crystallography [8]. For clarity of presentation only selected amino acids are shown in views A and B. Blue spheres, water molecules; magenta spheres, manganese ions (the labels A4, B3, C2 and D1 combine the crystal structure and the EPR based notations for these ions); red spheres, μ-oxo bridges; yellow sphere, calcium.

[14–16] (Fig. 2). The oxidizing equivalents are accumulated on four redox-active metal ions (manganese ions), with possible participation of ligands or oxo-bridges in the S_3 state. Having several redox active centers in the cluster reduces the reorganization energy for any specific metal site, allowing a concerted 4-electron reaction to occur in S_4 that avoids high-energy one-electron water-oxidation steps [13,17].

Information about water binding in the WOC has been obtained by several different techniques: X-ray crystallography (XRD) [8], magnetic resonance [4,18], FTIR difference spectroscopy [4,19], and membrane-inlet mass spectrometry [4,20–22]. A general problem for the identification of substrate water molecules is that water is not only the substrate, but also the 'solvent' of PSII. Therefore, isotope labeling in combination with suitable time-resolved experiments is necessary for discriminating between substrate and structural water molecules. In mass spectrometry and FTIR spectroscopy the mass difference between different oxygen isotopes (e.g. ^{16}O and ^{18}O) can be employed to monitor (substrate) water uptake/exchange by adding water in which the oxygen atom is labeled with ^{18}O. Magnetic resonance spectroscopy uses a similar approach, now introducing water where the oxygen is labeled with the ^{17}O isotope as it has a magnetic moment (spin of $I = 5/2$), while both ^{16}O and ^{18}O do not have a magnetic moment and are thus NMR/EPR silent. H_2O/D_2O exchange can also be useful, but this approach is less direct since it probes exchangeable protons rather than substrate oxygens.

The two substrate water molecules may each occur in three different protonation states when ligated to the Mn_4CaO_5 cluster, and their protonation state is expected to vary within the S_i state cycle. Despite this they will collectively be referred to as substrate waters in this review. Since the two substrate water molecules can be distinguished by their exchange rates (see below), they are commonly described as the fast (W_f) and slowly (W_s) exchanging substrate waters.

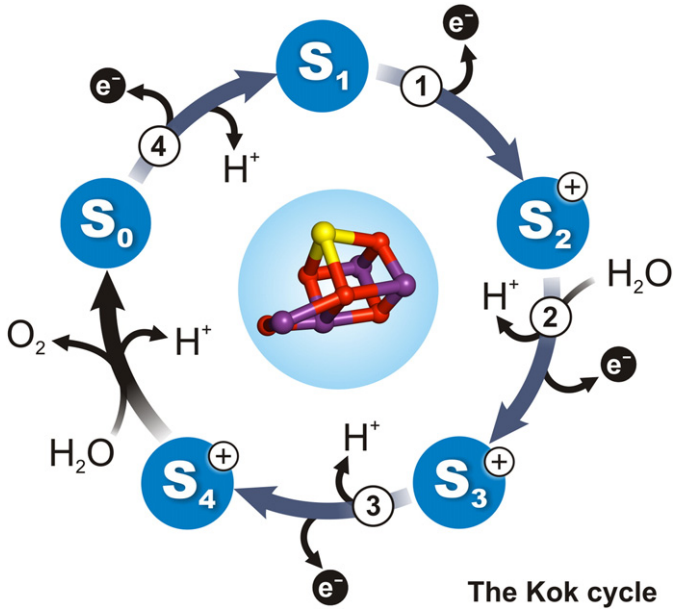

Fig. 2. Kinetic scheme (Kok cycle) describing the S_i state advancement by electron and proton removals from the WOC during water-splitting in photosystem II [12]. Water-binding within the cycle is based on FTIR data by Noguchi [64,86]. Both waters likely represent waters that become substrates in the next cycle ('next substrates').

2. Membrane-inlet mass spectrometry

Of the methods listed above, only time-resolved membrane inlet mass spectrometry (TR-MIMS) in combination with fast $H_2^{16}O/H_2^{18}O$ exchange is exclusively sensitive to substrate water. The reason for this is that this experiment measures the level of isotopic enrichment of the product, i.e. in the O_2 molecule released by PSII after a labeling and illumination event (see below), as opposed to the reactant, i.e. the large number of waters at or in the vicinity of the WOC (Fig. 1). However, TR-MIMS yields 'only' kinetic and no structural information. Therefore, on the basis of TR-MIMS data one can conclude whether or not a substrate is bound in a particular S_i state, and how fast it can exchange against bulk water, but not directly derive where or how it is bound. For a molecular understanding of substrate binding and exchange, kinetic correlations need to be established between substrate water exchange rates as measured by TR-MIMS and exchange rates observed by spectroscopic methods that are sensitive to specific oxygens (bound water molecules) within the WOC. While these correlations are in their infancy, much has already been learnt about the likely binding sites of the WOC by comparison to data collected in model systems [22] and by using structural information about the WOC as a guide [8,11,15,23–26].

In addition, S_i-state dependent changes of the substrate water exchange rates [27] can be related to S_i state dependent changes of Mn oxidation states and structural alterations (variation of Mn – Mn distances, see below) [15,28–30].

TR-MIMS is basically a pump probe technique. Dark-adapted PSII samples are flashed into the desired S_i state and then $H_2^{18}O$ is injected into the PSII suspension to induce a sudden jump in the $H_2^{18}O$ concentration. The equilibration of the bulk $H_2^{18}O$ into the substrate binding sites is then followed by analyzing the isotopic composition of the O_2 release in response to one or more flashes given after various incubation times (see Fig. 3C). In this way, the time course of exchange is probed point wise, where each time point corresponds to a new aliquot of the PSII sample. The time resolution is determined by the mixing time of $H_2^{18}O$ into the PSII suspension, which currently takes no more than 8 ms. Further details of the method and corresponding data analysis are described in recent reviews [31–34]. A typical result for substrate water exchange in the S_3 state of spinach thylakoids is shown in Fig. 3A and B. The exchange is followed at two mass to charge ratios:

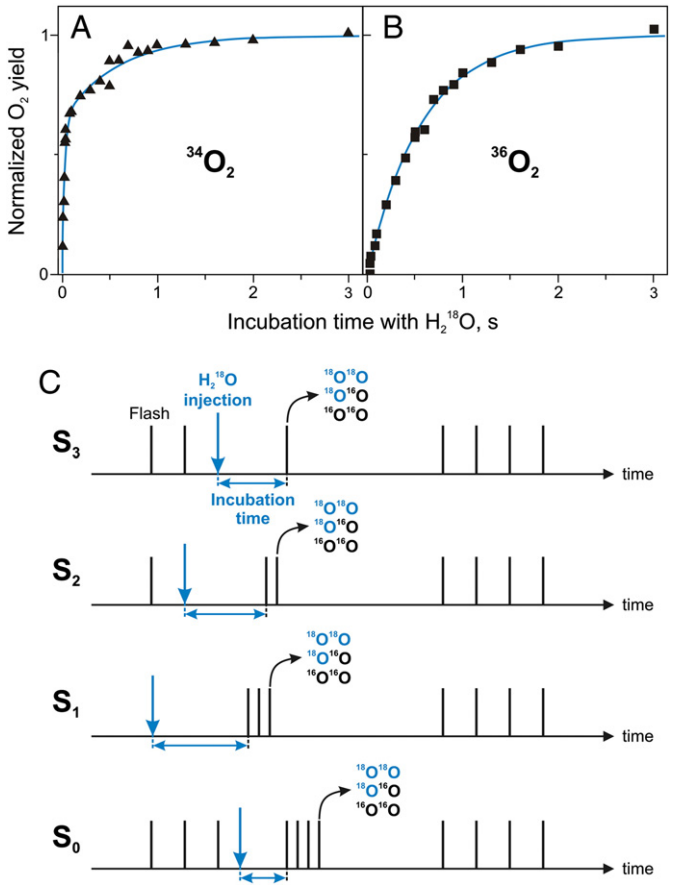

Fig. 3. Substrate-water exchange kinetics measured by time-resolved membrane-inlet mass spectrometry at $^{16}O^{16}O$ (m/z = 34, A) and $^{18}O^{18}O$ (m/z = 36, B) in the S_3 state of spinach thylakoids at 10 °C and pH 6.8. Black symbols are data points, while the blue lines represent biexponential ($^{34}O_2$, A) and monoexponential ($^{36}O_2$, B) fits, respectively. The slow phase in the $^{34}O_2$ data is fit with the same rate as determined for the $^{36}O_2$ data. Substrate water exchange rates measured in this way are listed in Tables 1–3. C: Flash-injection protocols for measuring substrate water-exchange in photosystem II by time-resolved isotope-ratio membrane-inlet mass spectrometry. Black vertical lines indicate excitations of the PSII sample with single turnover flashes, the blue arrow signifies the time of rapid $H_2^{18}O$ injection into the sample. Variation of the delay between $H_2^{18}O$ injection and the O_2 evolving flash sequence (incubation time) allows to point wise probe the kinetics of the substrate water exchange reaction. A group of 0–3 flashes at 2 Hz is used to excite the PSII sample into the desired S state. These preflashes are typically separated by 10 s from the subsequent 1–4 O_2-producing flashes, which are given at 100 Hz frequency. This frequency is a compromise between minimizing further water-exchange in the subsequent S states and allowing complete sample turnover into the next S state. The final group of four flashes is used to produce an O_2 signal employed for normalization.

m/z = 34 represents the singly labeled ($^{34}O_2$; Fig. 3A), and m/z = 36 the doubly labeled product ($^{36}O_2$; Fig. 3B). For $^{34}O_2$, only one of the two substrates exchanged, i.e. either W_f *or* W_s whereas for $^{36}O_2$ both W_f and W_s exchanged. A biphasic rise is seen for the $^{34}O_2$ signal as a function of the $H_2^{18}O$ incubation time at moderate final enrichments, suggesting that the two substrates have different exchange rates. As the $^{36}O_2$ signal requires both substrates to exchange, its rise is instead mono exponential, matching the rate of the slow rise seen for the $^{34}O_2$ signal. The monoexponential increase of the $^{36}O_2$ signal excludes sample heterogeneity as cause for the biphasic kinetics of the $^{34}O_2$ signal, proving that both substrate waters are bound in the S_3 state and that the two substrates, W_f and W_s, are bound in chemically nonequivalent ways [21,35]. Removal of all extrinsic proteins at neutral pH has only a marginal effect on the substrate water exchange kinetics: a 2–3 fold decrease of both exchange rates is reported [34,36]. This finding is very significant, since it demonstrates that the exchange rates are not limited by diffusion to the catalytic site, but rather by the energies of the transition states for their exchange.

Substrate water exchange has been probed in all stable S_i states [27]. Table 1 lists the rates of exchange for W_s and W_f for spinach thylakoids at 10 °C. These rates are abbreviated as k_s and k_f, respectively. In this context the ability to measure an exchange rate is proof for substrate water binding in the WOC. The data show that W_s is bound in all four stable S_i states (S_0, S_1, S_2, S_3), while W_f is bound (or is at least associated with the WOC) in the S_2 and S_3 states [37]. In the lower S-states the rate of exchange of W_f is faster than the time resolution of the experiment in the S_0 and S_1 states [13,22]. Although a rate cannot be measured it can still be inferred that W_f exchanges (or binds from bulk in the next S state transition), as the $^{34}O_2$ signal kinetic is offset from zero (in excess of 50% of the final signal), at the first time point (i.e. 8 ms).

Interesting variations in the exchange kinetics as a function of S_i state are observed. The most dramatic change is a 500-fold slowing of the exchange rate of W_s during the S_0 to S_1 transition [27,37]. This is most easily rationalized in a model where W_s is bound to the Mn center that is oxidized in this transition and in which W_s concomitantly loses a proton [13,27,28,33,38]. Unexpectedly, the rate at which W_s exchanges with bulk water increases 100-fold in S_2 as compared to S_1, and no further change is induced by S_3 state formation despite the known structural changes of the Mn_4CaO_5 cluster in this latter transition [27,39,40]. The exchange of W_f is about 3-fold slower in S_3 than in S_2 [37]. In addition, since the fast exchange becomes kinetically resolved for the first time in the S_2 state, there is likely a significant slowing of the exchange of W_f between the S_1 and S_2 states. If this is indeed the case, this would be consistent with W_f being a ligand of a Mn that is oxidized during this transition.

Biochemical Ca/Sr exchange leads to an almost 4-fold increase of k_s, while k_f is only marginally affected [41]. This finding is very important since it demonstrates that W_s is connected to Ca in the S_3 state. A similar increase of k_s is also found for the S_2 and S_1 states, implying that W_s is bound to Ca/Sr throughout the Kok cycle. The D1-D61N mutant decreases the rate of W_f exchange by a factor of 6.5, while slowing k_s by a factor of 3 [42]. In contrast, the D1-D170H mutation has only small effects on W_s and W_f [42]. It is interesting that the second sphere ligand D1-D61 has a larger effect on the water exchange rates than D1-D170, which is a direct ligand of the Mn_4CaO_5 cluster (Fig. 1). An 8.5 times

Table 1
S_i state dependence of substrate water exchange rates measured by TR-MIMS in spinach thylakoids [21,27,34,35,37] and Sr-substituted BBY [41].

S_i state	Ca (thylakoids)		Sr (BBY)	
	k_s, s^{-1}	k_f, s^{-1}	k_s, s^{-1}	k_f, s^{-1}
S_0	~10	>120	–	–
S_1	~0.02	>120	~0.08	>120
S_2	~2.0	~120	~9.0	>120
S_3	~2.0	~40	~6.0	~23

Table 2
Treatments affecting S_3 state substrate water exchange rates as measured by TR-MIMS in spinach samples at 10 °C.

condition	Sample type	k_s, s^{-1}	k_f, s^{-1}	Ref
H_2O, pH 6.8	Thylakoids	1.83 ± 0.17	38 ± 2	[34]
D_2O, pD 6.8	Thylakoids	1.94 ± 0.12	52 ± 2	[34]
H_2O, pH 5.0	Thylakoids	~1.8	~38	[34]
H_2O, pH 8.0	Thylakoids	~2.0	~43	[34]
H_2O, pH 6.8	BBY	2.5 ± 0.2	30 ± 2	[41]
H_2O, pH 6.8	BBY, Ca-depl. + $CaCl_2$	1.4 ± 0.1	27 ± 2	[41]
H_2O, pH 6.8	BBY, Ca-depl. + $SrCl_2$	5.8 ± 0.3	23 ± 5	[41]
H_2O, pH 6.8	BBY, −16, 23 and 33 kDa, plus $CaCl_2$	1.6 ± 0.7	10 ± 3	[36]

acceleration of the fast exchange was found in the CP43-E354Q mutant, which is also a direct ligand to the cluster [43]. The only mutation that affects W_s and W_f in opposite way is D1-H332Q: while W_s exchange is slowed 3-fold, the exchange rate of W_f is twice as large as compared to the wild type [44].

The strong effect of the second sphere mutation (D1-D61N) suggests that H-bonding is likely to be very important for the exchange of the fast substrate. This notion is strongly supported by H/D exchange measurements which show a negative H/D isotope effect of 0.63 (if extrapolated to 100%) for W_f, while k_s is unaffected by H/D exchange [34]. In contrast, the substrate water exchange rates vary little with pH in the range of pH 5.0 to pH 8.0 [34]. This striking discrepancy indicates that the internal pH (protonation state of the H-bonding network directly surrounding the Mn_4CaO_5 cluster) is very little affected by the outside pH in this range, a property potentially imparted by the three capping extrinsic proteins. Activation energies of 75 kJ mol^{-1} and 40 kJ mol^{-1} have been determined for the slow and fast exchange in the S_3 state of spinach thylakoids, respectively (Table 4) [21,34,35].

On a qualitative level these data have been interpreted by Hillier, Wydrzynski and Messinger to show that W_s is an oxo-bridge between Ca and Mn, while W_f is likely a terminal ligand to Mn [13,28,34,41]. The rational for this is that the exchange of W_s depends on Ca/Sr exchange, yet water exchange on Ca is known from model complexes to be orders of magnitude faster than k_s [21,22,33]. In addition, the strong S state dependence of W_s, especially during the $S_0 \rightarrow S_1$ transition, seems difficult to explain if W_s has no direct connection to Mn. In contrast, W_f is almost invariant to Ca/Sr exchange. On that basis terminal ligation to Mn is preferred over a Ca-ligand. Several alternative interpretations have been put forward by other authors, which will be addressed in part in the following sections in the context of new structural constraints [26,45–49].

3. Structure and S_i state dependent changes of the WOC

The recent 1.9 Å crystal structure of PSII includes more than 1300 water molecules per PSII monomer [8]. Most of these water molecules are located in the extrinsic luminal cap that is formed by luminal extensions of the psbB (CP47) and psbC (CP43) proteins, and by three extrinsic proteins: psbO (extr. 33 kDa), psbV (CytC550) and psbU (extr. 12 kDa). This arrangement protects and stabilizes the water-splitting Mn_4CaO_5 cluster and its two Cl^- cofactors [8,9,50]. Several water-filled channels

Table 3
Mutations affecting S_3 state substrate water exchange rates as measured by TR-MIMS in thylakoids of *Synechocystis* sp. PCC6803 at 10 °C.

Mutation	k_s, s^{-1}	k_f, s^{-1}	Ref
Synechocystis wt	0.47 ± 0.04	19.7 ± 1.3	[42]
D1-D61N	0.16 ± 0.02	3.0 ± 0.3	[42]
D1-D170H	0.70 ± 0.16	24 ± 5	[42]
D1-E189Q	0.9 ± 0.2	32 ± 5	[88]
CP43-E354Q	0.9 ± 0.4	170 ± 40	[43]
T. elongatus wt	0.40 ± 0.02	18.9 ± 1.0	[44]
D1-H332Q	0.015 ± 0.01	37 ± 5	[44]

Table 4
Activation energies for substrate water exchange in spinach thylakoids [21,34,35].

S_i state	$E_{A,s}$, kJ mol^{-1}	$E_{A,f}$, kJ mol^{-1}
S_0	–	–
S_1	83 ± 4	–
S_2	71 ± 9	–
S_3	78 ± 9	40 ± 5

have been identified within this luminal cap and variously assigned to support proton or O_2 release, and water access to the catalytic site [9,51–53]. Surprisingly many water molecules were found in the vicinity of the Mn_4CaO_5 cluster. These structural waters appear to form an ordered H-bonding network that shuttles protons away from the cluster [8,54]. They may also provide structural flexibility to the Mn_4CaO_5 cluster. Interestingly, one side of the cluster, the side along the Mn_{A4}–O_5–Mn_{D1} axis, appears to be 'dry' [8]. In addition to these protein-ligated waters and the five μ-oxo-bridges of the Mn_4CaO_5 cluster, the 1.9 Å crystal structure revealed that the Mn_4CaO_5 cluster has four terminal water ligands: W1 and W2 are bound to Mn_{A4}, while W3 and W4 are ligated to Ca.

Many of the Mn – O and Mn – Mn distances in this 1.9 Å XRD model of the WOC are longer than those obtained by extended X-ray absorption fine structure (EXAFS) spectroscopy (Table 5) [8,11,40]. This has been attributed to radiation-induced reduction of the cluster during X-ray crystallography [25,55–57], suggesting a Mn^{II} content of 25%; on average one Mn^{II} and likely 3 Mn^{III} per WOC [55]. According to the largely accepted high-valent oxidation state model, the dark-stable S_1 state contains two Mn^{III} and two Mn^{IV} ions per WOC, while four Mn^{III} ions (or $Mn^{II}Mn^{III}Mn^{III}Mn^{IV}$) are suggested for the S_1 in the low valent oxidation state model, which is supported by only a few groups [4,38,46,58–60]. All $S_i \rightarrow S_{i+1}$ state transitions may involve Mn^{III} to Mn^{IV} oxidations [38,40]. However, for $S_0 \rightarrow S_1$ a Mn^{II} to Mn^{III} oxidation is discussed also. In addition, there is a substantial set of experiments that have been interpreted to show that the oxo-bridges of the cluster take part in storing the redox equivalent accumulated during the $S_2 \rightarrow S_3$ transition [30,61].

Several attempts have been made to optimize the reduced crystallographic structure of the PSII complex to obtain structures for the S_1 and S_2 states. The models derived by the Siegbahn, Neese, Kusunoki and Batista groups that used the 1.9 Å crystal structure as starting point are all very similar, in contrast to earlier models [62]. Using the high valent option they all find that the central O5 moves to a normal bridging position between Mn_{A4} and Mn_{B3} and that all Mn – Mn and Mn – O distances are now in good agreement with EXAFS data. Such a model is schematically depicted in Fig. 4 (S_1, model A). Importantly, these models provide an excellent basis for explaining the EPR and ENDOR signals of the S_2 state. In contrast, Pace and Stranger find good agreement with the unusually long crystallographic Mn – O distances using the low valent option [23,25,26,54,58,62,63].

On the basis of EXAFS spectroscopy, S state-dependent structural changes within the cluster are known to occur during the $S_0 \rightarrow S_1$ and $S_2 \rightarrow S_3$ transitions. The $S_0 \rightarrow S_1$ transition is consistently described as involving a contraction of one Mn – Mn bond from 2.85 Å to about 2.7 Å [29,40], while no agreement has been reached for the $S_2 \rightarrow S_3$ transition. Both the formation of an extra 2.7 Å distance and the lengthening of

Table 5
Comparison of Mn – Mn and Mn – O/N distances in the dark-adapted WOC as determined by X-ray crystallography [8] and EXAFS [11,29,79,95–97] (for comparison see also [40,98,99]).

Number of distances	XRD, Å	EXAFS, Å
Mn – O/N	2.2	1.87
3 Mn – Mn	2.8–3.0	2.7–2.8
1 Mn – Mn	3.3	3.3
3 Mn – Ca	3.3–3.5	3.4
1 Mn – Ca	3.8	3.9

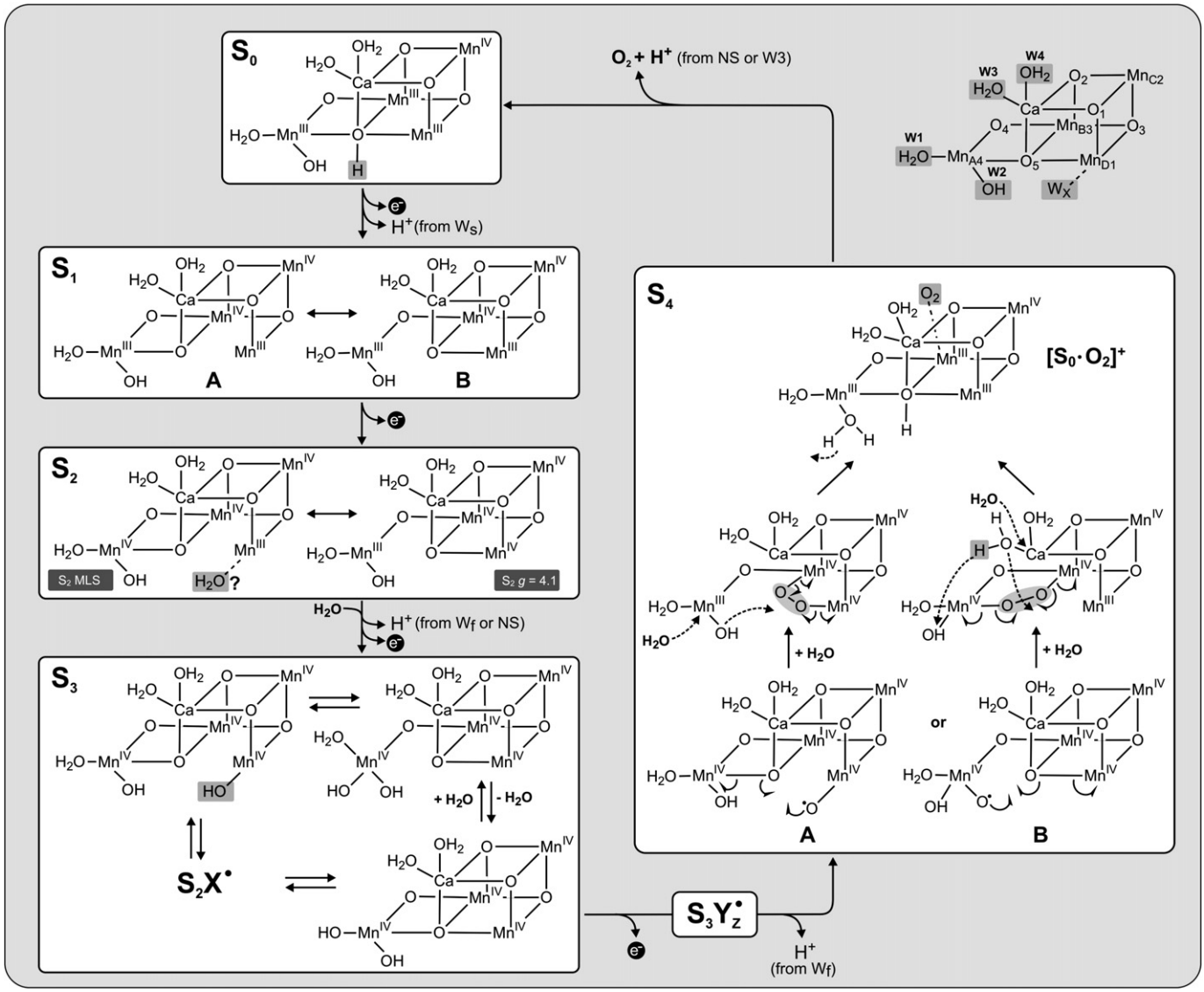

Fig. 4. Molecular interpretation of S_i state advancements and suggested mechanism for O–O bond formation in photosystem II. In line with evidence described in the text it is suggested that the Mn_4CaO_5 cluster can attain various almost isoenergetic structures in the S_1 to S_3 states. O–O bond formation mechanism A is a schematic representation of Siegbahn's proposal that is based on the 'S_2 MLS' configuration of the WOC [24,38,54], while mechanism B employs the 'g = 4.1' configuration and is an update of an earlier proposal by Messinger [28,83]. $S_2X^{\bullet}$ represents the possibility of an S_3 state in which the Mn ions attain the same oxidation states as in the S_2 state and the oxidizing equivalent is stored as a radical (X = oxo bridge, histidine or Y_Z; see text). $S_3Y_Z^{\bullet}$ is a kinetic intermediate prior to O_2 evolution that has been identified from a lag phase in UV and EPR transients following $Y_Z^{\bullet}$ reduction, O_2 release kinetics, transient X-ray absorption measurements and by time-resolved FTIR spectroscopy. The consensus interpretation of these experiments is that the Mn_4CaO_5 cluster is only oxidized from S_3 to S_4 by $Y_Z^{\bullet}$ after a proton has been released from the water-oxidizing complex [100–105]. Similar intermediates exist between the other S state transitions, but are not shown because they are too short lived. Details about the suggested mechanisms are described in the text.

Mn – Mn distances have been reported [39,40]. FTIR measurements indicate changes in the ligands during the $S_1 \rightarrow S_2$ transition [64,65], but no substantial structural changes within the cluster were detected by EXAFS. This discrepancy maybe explained by the fact that in this transition no proton is released from the WOC. The changes observed by FTIR may therefore reflect the response of the protein pocket to this extra positive charge.

4. Structural flexibility of the Mn_4CaO_5 cluster

S_1, S_2 and S_3 states may exist at room temperature in various sub-states, which differ in protonation pattern, oxidation state distribution and/or their overall structural conformation [17,26,45,58,63,66,67]. Gernot Renger was likely the first to propose a multi-state model, specifically for the S_3 state. He suggested that a redox equilibrium exists between Mn ions and substrate water leading to the formation of a peroxidic intermediate in a certain fraction of centers, and that this fraction may exist in two tautomeric forms [17,67]. Later, Kusunoki proposed on the basis of DFT calculations various tautomers of the S_1 state that differ in structure. A subset of these resembles the 1.9 Å crystal structure [26,45]. A similar idea was advanced by Pace and Stranger, as a means of rationalizing differences between various low resolution models derived from X-ray crystallography [58,63].

Perhaps the best suggestion that structural heterogeneity is an intrinsic feature of the WOC is the recent study of Pantazis and coworkers. This study ties structural variation with the well-known variation in magnetism seen for the WOC in the S_2 state. Specifically, it was shown that the S_2 EPR multiline (MLS) and the S_2 g = 4.1 signals derive from two different structures, which differ in terms of the position of the central O5. At the experimental temperatures of about 10 K O5 can occupy either a bridging position between Mn_{A4} and Mn_{B3} (MLS) or complete the Mn_3CaO_4 cube, leaving the Mn_{A4} connected to Mn_{B3} via a mono μ-oxo bridge (S_2, Fig. 4), with the g = 4.1 configuration resembling closely an earlier structural suggestion [28]. This structural difference

is coupled to a redox isomerism between $Mn^{IV}_{A4}Mn^{III}_{D1}$ and $Mn^{III}_{A4}Mn^{IV}_{D1}$ and the energy difference between the two conformations was calculated to be small (about 1 kcal mol^{-1} in favor of the MLS state) [66]. As discussed below, at room temperature a dynamic equilibrium between these two states may exist that also contributes to the unusually fast isotopic exchange of O5, and the 100 times increase in exchange rate in S_2 as compared to the S_1 state [66]. Pantazis et al. also suggest that the g = 4.1 state configuration may be able to advance to the S_3 state [66]. This possibility is explored in Fig. 4.

5. S_3 state water-exchange

Assuming the high-valent Mn oxidation state model and Mn-centered oxidations during all S_i-state oxidations, all four Mn ions in the S_3 state are in oxidation state Mn^{IV}. No experimental exchange rates for terminal water or hydroxo ligands to Mn^{IV} have been reported in the literature. Exchange of terminal waters or hydroxo groups has been suggested to be significantly slower for Mn^{IV} as compared to Mn^{III} on the basis of a qualitative comparison with exchange data on other metals [33]. However, a recent theoretical study finds that if the total charge of the complex is kept neutral by adding appropriate ligands, the activation energies for water exchange and therefore the exchange rates for terminal waters on Mn^{III} and Mn^{IV} are both in the range of those for the fast exchanging substrate water in the S_2 and S_3 states [48]. Two experimental studies indirectly agree with this conclusion. Tagore et al. reported for both a bis-μ-oxo bridged $Mn^{III}Mn^{IV}$ complex and its corresponding $Mn^{IV}Mn^{IV}$ complex only the exchange rates of the oxo-bridges. In contrast, for both complexes the two terminal waters were lost from the parent ions during ionization in the ESI-TOF experiments, indicating a rather weak binding (good exchangeability) as compared to the bridges [68,69].

The activation energy for the exchange of oxo-bridges in bis-μ-oxo bridged $Mn^{IV}Mn^{IV}$ dimers was calculated to be very close to that measured for the exchange of W_s in PSII [48]. However, measurements on $Mn^{III}Mn^{IV}$ dimers and $Mn^{IV}Mn^{IV}$ dimers report exchange rates that are 10^4–10^5 times, respectively, slower than in PSII [68,69]. It is important to note that these rates are measured with very low water concentrations in organic solvents and therefore likely significantly underestimate the absolute magnitude of the exchange rate as compared to PSII. However, also the difference in relative rates between the synthetic $Mn^{III}Mn^{IV}$ and $Mn^{IV}Mn^{IV}$ complexes appears to be in contrast to the finding in photosystem II where the slow substrate is exchanging with almost exactly the same rate and activation energy in S_3 (often depicted as $(Mn^{IV})_4$) as in S_2 ($Mn^{III}(Mn^{IV})_3$; Tables 1 and 4).

An easy way out would be to assume that the high-valent oxidation states are incorrect, and that the oxidation states of S_3 are rather $(Mn^{III})_2(MnIV)_2$ [58,59]. However, as pointed out above, there appears to be too much evidence against the low oxidation state option to further consider this idea here.

Two other possibilities are suggested to explain the invariance and magnitude of the slow water exchange rates in the S_2 and S_3 states (the fast water is not further discussed since exchange rates appear to be in the right order of magnitude for Mn^{III} and Mn^{IV}, see above). i) The slow substrate is coordinated to Mn^{IV} ion(s) in both S_2 and S_3, which via structural isomerism (described above; Fig. 4) allows it to interchange with another, more fast exchanging ligand site(s) within the complex, i.e. the bridge interchanges with a terminal ligand. Such an equilibrium is shown for the S_3 state in Fig. 4, but can also occur starting from the g = 4.1 state in S_2. To rationalize the similar rates in S_2 and S_3 one simply needs to assume that these equilibria have low barriers and therefore occur at rates that are fast as compared to the W_s exchange. ii) Similarly, these findings may indicate that in both S states basically the same transition state for W_s exchange can be reached, which would mean that the Mn_4CaO_5 cluster can attain in the S_3 state at room temperature a state that resembles in both Mn-oxidation state and dynamics the S_2 state. For this to happen the $(Mn^{IV})_4$ state would need to be in equilibrium with one or more other states in which one oxidizing equivalent is stored in form of a radical. In that case the exchange may occur in the fraction of centers that are in this radical state in a similar way as in the S_2 state. In order not to alter the overall exchange rate, this alternative requires a fast redox equilibrium between $Mn^{IV}X$ and $Mn^{III}X^{\bullet}$. Options for X discussed previously in the literature include the formation of an oxo bridge radical or the oxidation of a histidine ligand (e.g. D1-H332) [28,30,70]. One additional attractive possibility is a redox equilibrium with Y_Z, which was suggested for example to explain the high miss parameter of the $S_3 \rightarrow S_0$ transitions [71–73] (see however [74]).

6. Deduction of possible substrate binding sites

As the 1.9 Å crystal structure exhibits four terminal water-derived ligands with suitable geometry for O–O bond formation, the crystal structure on its own does not allow the identification of the two substrate molecules and of the mechanism of water oxidation. The situation is further complicated by the fact that oxo-bridges may also be involved in O–O bond formation. As such, several different, structurally consistent mechanisms are still discussed including: the coupling of the two terminal water-derived ligands on the outer Mn_{A4} [26,45], nucleophilic attack of the Ca-bound W_3 onto a terminal oxo formed during the S state cycle from W_2 [8,75,76], nucleophilic attack of the Ca-bound W_3 (water or HO^-) onto O5 [8,77–79], radical coupling of W2 with O5 [75], and radical coupling between O5 and a terminal oxyl-radical formed in the S_4 state on Mn_{D1} from a non-crystallographic water W_x, which is suggested to first bind to Mn_{D1} as terminal hydroxo ligand during the $S_2 \rightarrow S_3$ transition [24,54].

Below the structure of the WOC will be used together with the TR-MIMS data and spectroscopic information for the assignment of the two substrate binding sites. The deduction begins with the assignment of W_s, since the slow water is involved in the largest S_i state dependent change observed in the TR-MIMS measurements: its exchange rate is slowed by a factor of 500 during the $S_0 \rightarrow S_1$ transition. In addition, its exchange rate is altered significantly by Ca/Sr substitution. Subsequently, possible sites for W_f will be analyzed.

6.1. The slowly exchanging W_s

Ca/Sr substitution increases the slow rate of exchange in all S_i states, but preserves the pattern of the unusual S_i state dependence (Tables 1, 2 and [41]). As discussed above, this provides strong evidence for the direct ligation of W_s to Ca *and* Mn. Thus, from comparison to the crystal structure, three candidates exist for W_s: O1, O2 and O5, i.e. all bridges between Ca and Mn ions. Recently, electron nuclear double resonance detected NMR (EDNMR) spectroscopy experiments at W-band frequency have demonstrated that there is only one exchangeable bridge at up to 1 hour incubation time with $H_2^{17}O$ buffer, and that this bridge is either O4 or O5 [77] (see also [80,81]). Therefore, O1, O2 and O3 can be excluded as substrates based on EDNMR, and O4 since it is not ligated to Ca. This analysis thereby identifies O5 as the slowly exchanging substrate water. A structurally equivalent position for W_s was suggested previously on the basis of analogous arguments using earlier structural models for the WOC [13,28,38], and on the basis of DFT calculations [24,82,83]. An alternative explanation for the unusual S-state dependence of k_s is indirect modulation via H-bonding. This would increase the number of candidates for W_s, for instance W3 and W2 would become options. However, this scenario appears unlikely because of the absence of an H/D isotope effect for k_s, in contrast to the H/D effect on the exchange of W_f.

The assignment of W_s to an oxo-bridge has been challenged on the basis of water exchange rates of oxo bridges in model systems [68,69]. Such oxo-bridge exchange rates are in models typically several orders of magnitude slower than found for W_s and W_f. It is therefore highly important that the above described EDNMR experiments were also

performed using a rapid mix-freeze approach. These data show that the oxo-bridge (O5) exchanges rapidly: complete exchange was observed in the S_1 state within 10–15 s (the shortest mixing time achieved). This strongly supports the suggestion that O5 is indeed a substrate water. However, improved time resolution and experiments in at least the S_1 and S_2 states or Ca- vs. Sr-PSII will be required to demonstrate that O5 is indeed W_s.

The trends in the S_i state dependence of the exchange rates further strengthen the assignment of O5 to W_s, as EPR, EXAFS and XRD data provide a simple rationale for the 500-fold slowing of the exchange rate during the $S_0 \rightarrow S_1$ transition [13,17,28,38]. If one assumes that O5 is protonated in the S_0 state, i.e. $W_s = O5(H)$ (S_0 state in Fig. 4), and that both Mn_{A4} and Mn_{B3} are in oxidation state III in S_0 such that O5(H) is bound at the Jahn–Teller axes of the two Mn^{III} ions, then from comparison to model Mn complexes oxidation of Mn^{III}_{B3} will slow the exchange of W_s due to a large decrease in the pK_a of the bridging oxygen, such that it is fully deprotonated in S_1 (i.e. an oxo-bridge). Concomitantly a bond length contraction of the Mn^{IV}_{B3}–O5 bond is also expected and indeed observed by EXAFS for PSII; the Mn–Mn vector, likely Mn_{A4}–Mn_{B3}, shortens from 2.85 Å in S_0 to 2.7 Å in S_1 [29,40]. As demonstrated earlier, such a structural change is also consistent with EPR and ^{55}Mn-ENDOR data of the S_0 and S_2 multiline states [38].

During the $S_1 \rightarrow S_2$ transition another Mn^{III} to Mn^{IV} oxidation occurs, but no proton is ejected into the lumen (Figs. 2 and 4). A further slowing of the exchange of W_s may be expected if now Mn_{A4} is oxidized, or no change at all if Mn_{D1} is oxidized. Instead, an increase of the exchange rate of W_s by a factor close to 100 is observed. This would be best explained by a significant structural change within the Mn_4CaO_5 cluster between the S_1 and S_2 states; however, such a change is not observed by EXAFS spectroscopy at 10 K. While a detailed exchange mechanism still needs to be worked out, one may speculate that the unusually fast exchange of O5 is due to its ability to interchange with another oxygen site within the complex such as the two terminal waters on Mn_{A4} or the two terminal waters on Ca, via structural isomerism as discussed above, i.e. S_2 MLS and g = 4.1 states (Fig. 4) [13,28,66]. This same pathway for exchange must not be present in S_1.

Another challenge is to explain as to why the exchange rate of W_s remains unaffected by the structural and oxidation state changes during the $S_2 \rightarrow S_3$ transition. As discussed above, the presently best suggestion is that the exchange mechanism involves a structural and/or redox equilibrium that may also include a $Mn^{III}Mn^{IV}Mn^{IV}Mn^{IV}$ radical state that allows water exchange to occur like in the S_2 state (Fig. 4; see also [17,84,85]).

6.2. The fast exchanging W_f

Accepting for now that $W_s = O5$, what are then the options for W_f? Assuming no major structural rearrangements upon going from the S_2 to the S_4 state, then of the two Ca-bound waters, only W3 is in a suitable position for O–O bond formation with O5 (Fig. 1) [8]. However, this assignment is unlikely, because of the very small effect of Ca/Sr substitution on W_f. Furthermore, the strong S_i state dependence of k_f that changes from a rate being unresolvable in S_0 and S_1 to one that is only 20 times faster than k_s, does not favor Ca as binding site of W_f. Therefore, W_f must be either W1 or W2, of which W2 appears to be in a much better geometric position for O–O bond formation with O5 (Fig. 1) [8]. This assignment is also consistent with W_f becoming detectable in the S_2 state for the first time, as Mn_{A4} is likely oxidized during the $S_1 \rightarrow S_2$ transition [54]. The marginal subsequent slowing (factor ~3) of W_f exchange upon S_3 formation is also consistent with this assignment, since in S_3 the last Mn^{III}, Mn_{D1} distal to W2, is expected to be oxidized (in the static low temperature picture; see Fig. 4) [54]. Therefore, the assignment of W2 as W_f appears to be fully consistent with such a qualitative analysis of the experimental data.

One alternative to this assignment was suggested by Siegbahn on the basis of DFT calculations. Siegbahn proposed that a non-crystallographic water (here termed W_x) binds very weakly near Mn_{D1} in the S_2 state, which becomes a ligand to Mn_{D1} in form of a hydroxo in the S_3 state [54]. In the S_0 and S_1 states W_x is suggested to be part of the 'sea' of waters around the cluster, thereby escaping its crystallographic detection near Mn_{D1}. This theoretical option is interesting, since it leads to an elegant suggestion for O–O bond formation with to date the lowest energy barrier. It is remarked though that in this model the exchange rate of W_x should strongly decrease between S_2 and S_3, i.e. more than by a factor of 3, and that W_x would need to bind in an area of the Mn_4CaO_5 cluster that contains, for reasons to be explored, no water molecules in the crystal structure.

7. Water-binding to the WOC during the $S_2 \rightarrow S_3$ transition

TR-MIMS data show that both substrate water molecules are bound already latest in the S_2 state [37]. This result appears to contradict data which comes from FTIR difference spectroscopy. Noguchi and coworkers have two strong lines of evidence suggesting water binding to the WOC during the $S_2 \rightarrow S_3$ and $S_3 \rightarrow S_0$ transitions. The first is based on the observation that the miss parameters for the $S_2 \rightarrow S_3$ and for $S_3 \rightarrow S_0$ transitions increase strongly upon partial dehydration [19]; the other on the observation of negative bands at about 1240 cm^{-1} in $D_2^{16}O$-minus-$D_2^{18}O$ double difference spectra for the $S_2 \rightarrow S_3$ and $S_3 \rightarrow S_0$ transitions that have no clear counter parts in other transitions [86]. When comparing these spectroscopic results to TR-MIMS data it is important to remember that spectroscopy is sensitive to the total hydration of the complex, whereas TR-MIMS only monitors the two substrate waters. Thus, the most straight forward interpretation is that the water bound upon $S_2 \rightarrow S_3$ is not a substrate, but rather a structural water, which likely becomes the substrate in the next cycle (next substrate, NS in Fig. 4). However, fast internal isotopic equilibration in the S_3 state between this newly bound water and W_f may lead to a situation in which it is impossible to make such a clear distinction. The critical point from these FTIR studies is that a *change* in the total solvation of the Mn_4CaO_5 complex upon the $S_2 \rightarrow S_3$ transition is required for water splitting catalysis to occur. Thus far, only the Siegbahn model has explicitly included a change in the complex's solvation during the $S_2 \rightarrow S_3$ transition.

This increase in the net solvation, in which the next substrate is already preloaded into the complex, is suggested to be important for the proton release during the $S_2 \rightarrow S_3$ transition and for the O_2 release step in the $S_4 \rightarrow S_0$ transition. It is expected that the release of O_2 and the refilling of the vacant substrate sites occur as a concerted process [20], which is facilitated by having the next substrate(s) already bound to metal ions of the Mn_4CaO_5 cluster (Fig. 4, S_4 state) [13].

8. Effects of mutations

One promising way of probing the substrate binding sites at the Mn_4CaO_5 cluster is studying how site directed mutants affect the substrate water exchange rates. Such experiments were performed either using *Synechocystis* sp. PCC6803 (D1-D61N, D1-D170H, D1-E189Q and CP43-E354) or *Thermosynechococcus elongatus* (D1-H332Q) as the model organism [42–44,87,88]. The results (Table 3) will be discussed below in relation to the structural models in Figs. 1 and 4, and with regard to the assignments made above for W_s and W_f. A caveat is that these models do not represent the S_3 state for which most of the experimental data in Tables 1–4 were obtained. Similarly, crystal structures for these mutants are not yet available. For clarity of presentation the effects of mutations will be discussed first employing the assumption that $W_f = W_2$. This is followed by a briefer discussion of the option $W_f = W_x$, to which the same principles apply.

The D1-D61 side chain is not a ligand of the Mn_4CaO_5 cluster, but is often discussed to be crucial for proton release from the WOC

[8–10,54,89]. It is therefore somewhat surprising that its mutation to asparagine (D1-D61N mutant) clearly affects both the fast and the slow exchange rates: the exchange of W_f and W_s is slowed by factors of 6.5 and 3, respectively [42]. The 1.9 Å crystal structure shows that D1-D61 and W1 form a H-bridge. D1-D61 is also connected to O4 via another water molecule (Fig. 1) [8]. The latter point is interesting since O4 is in trans position to W2 and may thereby affect its exchange. The D1-D61N mutation can be expected to strongly alter the H-bonding network around Mn_{A4} and may also lead to a situation that fewer waters are held in a favorable position for exchange with W1 or W2. The clear decrease of the fast exchange rate k_f in the D61N mutant is therefore consistent with the assignment of W_f to W2 or W1, of which W2 is favored for geometrical reasons (see above). The sensitivity of W_f exchange to mutations affecting the H-bonding network is unsurprising since k_f is sensitive to H/D exchange (Table 2). The effect of the D1-D61N mutation on W_s is likely transduced to O5 (W_s) via W1, which binds in the S_2 MLS configuration trans to O5 (Figs. 1 and 4). Changes around Mn_{A4} may also affect redox and structural equilibria mentioned above and thereby affect the exchange rate of O5.

D1-D170 bridges Mn_{A4} and Ca, and thereby is a direct ligand to Mn_{A4} [8,9]. Surprisingly, its mutation to histidine has almost no effect on the fast exchange, and speeds up the slow exchange only by a factor of 1.5 [42]. The structural alterations induced by this mutation are not easy to predict. His ligation to Mn instead of aspartate should lead to an increased charge at the cluster. This would certainly block the S_i state transitions and change water exchange rates; both are not observed. Alternatively, one may suggest that in place of D1-D170 a hydroxide ion binds between Mn_{A4} and Ca. Such an arrangement conserves the overall charge and the structure of the cluster [90]. D1-H170 would in that case not be a ligand to Mn or Ca. The surprising invariance of both exchange rates can then be understood, since basically identical Mn – Mn and Mn – Ca distances were calculated. If D1-H170 does not get in the way, also the H-bonding network around Mn_{A4} remains likely intact, so that also the fast exchange of W_2 (W_f) stays the same, as observed. The fact that the D170/HO^- ligation is perpendicular to the plain in which W1, W2 and O5 bind (cis position) is a further argument as to why the changes can be expected to be small [48].

CP43-E354 bridges Mn_{B3} and Mn_{C2}, and as a consequence is a trans ligand of O5. Its mutation to Q may therefore be expected to lead to a strong slowing of the exchange of W_s, since a negatively charged amino acid is exchanged against a neutral one. However, k_s is two times faster in this mutant [43,87]. This does not favor O5 as W_s, but on the other hand does not exclude it either, since the precise structure of this mutant in the S_3 state is unknown. As discussed for the D1-D170N mutant, there may be a compensating effect such as hydroxide binding. In addition, O5 is not only ligated by Mn_{B3}, but also by Ca, Mn_{A4} and/or Mn_{D1}. Therefore, the effect of this mutation on the energy of the transition state for water exchange is complicated to predict. More surprising is the finding that the exchange of W_f is increased by 8.5 times [43,87]. According to the crystal structure and the theoretical models no terminal water-ligand is bound to Mn_{B3} and Mn_{C2} (however, water-binding to one of these ions is consistent with FTIR data of this mutant) [8,23,24,91]. Therefore, there are three possible explanations: i) O5 is indeed the fast and not the slow substrate, but this seems unlikely on the basis of the above considerations; ii) the mutation restructures the H-bonding network in a way that W1 or W2 can be exchanged faster. This is possible, but only a rather indirect H-bonding network is seen in the 1.9 Å crystal structure between these two sites of the Mn_4CaO_5 cluster [8,54]; iii) the O4 bridge is modified, for example by breaking its H-bond to CP43-R357. This may strengthen the Mn_{A4} – O4 bond and thereby weaken the bond to W2 (W_f).

The D1-H332Q mutant is interesting for two reasons. Firstly, it is so far the only mutant that alters the fast and slow exchange in opposite ways: k_f is increased 2-fold, while k_s is slowed by a factor of 3 [44]. Secondly it targets the Mn_{D1} site of the cluster. Mn_{D1} is on the one hand a possible ligand to O5 ($g = 4.1$ structure, Fig. 4) [8,66], and on the other hand the proposed binding site of W_x (in the S_2 MLS configuration) [24,54,82]. The slowing of k_s is of similar magnitude (factors 2–4) as the increase of exchange rate in the D1-D170H (ligand of Mn_{A4}) and CP43-E354Q (ligand of Mn_{B3}) mutants, and after Ca/Sr exchange. It is interesting to note that O5 is the only oxygen surrounded by all these atoms. This leads to the suggestion that O5 (W_s) is in the S_3 state either directly or indirectly, e.g. via dynamic equilibria, connected to all the four metals (3Mn and the Ca), so that all four metals are able to affect the transition state energy of W_s exchange to a similar extent (positively or negatively). The increase in the fast water exchange rate as compared to the wild type (wt) may then be an indirect effect (if $W_f = W_2$).

Similar arguments can be made for $W_f = W_x$. While it is easier to understand the effects of the D1-H332Q and the D1-D170H mutations on W_x as compared to W2, the opposite is true for the D1-D61N mutant. No obvious H-bonding network is found in the 1.9 Å structure between D1-D61 and MnD1. However, the computational model of Siegbahn does have such a connection via D1-K317, Cl^- and two waters (Figure 2 in ref [54]). The strong effect of the CP43-E354Q mutant on W_f is also in case of $W_f = W_x$ very difficult to understand without further structural information about the mutant.

The uncertainty about the molecular interpretation of the mutant data is reminiscent to problems encountered when trying to localize Mn oxidation state changes during S state transitions within the Mn_4CaO_5 cluster by a combination of mutagenesis and FTIR spectroscopy [92,93]. The complex appears to be too coupled to allow simple and straight forward conclusions without detailed structural information on the mutants. However, two observations are of general importance: 1) in most cases the exchange rate of W_f is equally or more strongly affected than the exchange rate of W_s, and 2) the change in rate is—with one exception—for both substrate waters always in the same direction, i.e. if k_f increases, so does k_s, and if k_f decreases, so does k_s. The latter finding supports the notion of Kusunoki that W_s cannot only exchange directly with bulk water, but also via exchange with W_f. On that basis Kusunoki proposed the mono Mn mechanism, in which $W_1 = W_f$ and $W_2 = W_s$ [26,45]. This analysis is highly important, since it can, if correct, demonstrate that: i) W_f is already bound in the S_1 state; and ii) show that W_f is likely bound to the same metal as W_s; this would also be the case for W2 and O5 assuming the S_2 MLS configuration (Fig. 4).

In summary, of the waters and oxo-bridges resolved in the 1.9 Å crystal structure W2 and O5 emerge as the most likely candidates for W_f and W_s, respectively. A further possibility for W_f is a non-crystallographic water molecule that may bind in the vicinity of Mn_{D1} weakly in the S_2 state, and directly to Mn_{D1} in the S_3 state. Further work is required to firmly distinguish between these two options experimentally and to understand how the O – O bond is formed. A view is emerging that structural flexibility may be a key factor in these processes [17,26,45,58,63,66,67].

9. Evaluation of current mechanistic proposals

The reflections presented in this paper appear to exclude the nucleophile attack mechanisms in which Ca bound water attacks a terminal oxo or a μ-oxo bridge. Similarly, mechanisms involving two oxo-bridges, or two terminal waters are highly unlikely. What remains are two options involving O5 as W_s. In option A (Fig. 4) W_f is a water proposed on the basis of DFT calculations ($W_f = W_x$), while in option B W_f is W_2, i.e. a terminal hydroxo ligand to Mn_{A4}. Very interestingly, option B is based on the $g = 4.1$-like form of the cluster in the S_3 state so that the chemistry occurs near Mn_{A4}. In contrast, option A is based on an MLS-type configuration so that the chemistry occurs on the more secluded site near Mn_{D1}. Possible reaction mechanisms based on these two options are presented in Fig. 4 (S_4 state).

Option B is in line with suggestions based on the 1.9 Å crystal structure that the O – O bond formation may involve W2, W3 and/or

O5 [8]. Similarly, Barber, Brudvig and Batista suggested O–O bond formation in that 'corner' of their somewhat different cluster. Their proposals were based, however, on the nucleophilic attack mechanism between a Ca bound water and a terminal oxo on Mn_{A4} [10,76,94], which is strongly disfavored by the analysis presented in this review. Messinger used a modified model of the Barber structure, which strongly resembles the recently suggested g = 4.1 configuration, and proposed using similar arguments as in this paper that O–O bond formation may occur between a hydroxo bound to Mn_{A4} and the μ_3-oxo bridge between Ca and two Mn ions in the cube (equivalent to O5 between Mn_{B3} and Mn_{D1}) [28]. Subsequently, Siegbahn proposed the principle of his current O–O bond formation mechanism (which involves the S_2 MLS configuration) using a g = 4.1-type DFT model. A key aspect of Siegbahn's proposal is that a α,β,α,β spin configuration between the two Mn ions and the two substrate oxygen's reduces the activation energy for O–O bond formation significantly [82].

The advantage of side B is the good accessibility of water and of groups that can accept and shuttle away protons during the S state cycle, while an attractive feature of mechanism A is that the oxygen radical can be formed in a more hydrophobic environment. For mechanism A Siegbahn found a transition state for O–O bond formation that is clearly lower in energy than for a mechanism similar to option B that he studied previously [54,83]. Nevertheless, the evidence collected in this review calls for a further careful evaluation of both options by experiments and large scale theoretical studies. If indeed the barrier for interconversion between MLS-type and g = 4.1 type configurations in S_3/S_4 is also small, then the g = 4.1 state configuration may facilitate substrate binding during the $S_2 \rightarrow S_3$ transition, which upon rearrangements returns in S_4 to a Siegbahn like transition state allowing low energy barrier O–O bond formation—the best of both worlds.

Acknowledgements

We would like to thank William Ames, Alain Boussac, Warwick Hillier, Jan Kern, Takumi Noguchi, Dimitrios Pantazis, Gernot Renger, Dmitriy Shevela, Per Siegbahn, Tom Wydrzynski, Vittal Yachandra and Junko Yano for insightful discussions. In particular, it is acknowledged that William Ames championed the idea of the equilibrium between MLS and g = 4.1 like configurations in all S_i states. We are grateful to Dmitriy Shevela for preparing the figures, and to Håkan Nilsson for performing the water exchange experiments shown in Fig. 2 and to Gernot Renger for critical reading of the manuscript. Financial support was provided by Vetenskapsrådet, Energimyndigheten, the Strong Research Environment Solar Fuels (Umeå University), the Artificial Leaf Project Umeå (K&A Wallenberg foundation), and the Kempe foundation.

References

[1] A.W. Rutherford, A. Osyczka, F. Rappaport, Back-reactions, short-circuits, leaks and other energy wasteful reactions in biological electron transfer: redox tuning to survive life in O_2, FEBS Lett. 586 (2012) 603–616.
[2] G. Renger, Light induced oxidative water splitting in photosynthesis: energetics, kinetics and mechanism, J. Photochem. Photobiol. B: Biol. 104 (2011) 35–43.
[3] G. Renger, Primary processes of photosynthesis. Principles and apparatus, in: D.-P. Häder, G. Jori (Eds.), Comprehensive Series in Photochemical and Photobiological Sciences, The Royal Society of Chemistry, Cambridge, 2008.
[4] J. Messinger, T. Noguchi, J. Yano, Photosynthetic O_2 evolution, in: T.J. Wydrzynski, W. Hillier (Eds.), Molecular Solar Fuels, RSC, London, 2012, pp. 163–207.
[5] J.P. McEvoy, G.W. Brudvig, Water-splitting chemistry of photosystem II, Chem. Rev. 106 (2006) 4455–4483.
[6] H. Dau, I. Zaharieva, Principles, efficiency, and blueprint character of solar-energy conversion in photosynthetic water oxidation, Acc. Chem. Res. 42 (2009) 1861–1870.
[7] T. Wydrzynski, K. Satoh, Photosystem II. The light-driven water:plastoquinone oxidoreductase, in: Govindjee (Ed.), Advances in Photosynthesis and Respiration, Springer, Dordrecht, 2005.
[8] Y. Umena, K. Kawakami, J.R. Shen, N. Kamiya, Crystal structure of oxygen-evolving photosystem II at a resolution of 1.9 Å, Nature 473 (2011) 55–61.
[9] A. Guskov, J. Kern, A. Gabdulkhakov, M. Broser, A. Zouni, W. Saenger, Cyanobacterial photosystem II at 2.9 Å resolution and the role of quinones, lipids, channels and chloride, Nat. Struct. Mol. Biol. 16 (2009) 334–342.
[10] K.N. Ferreira, T.M. Iverson, K. Maghlaoui, J. Barber, S. Iwata, Architecture of the photosynthetic oxygen-evolving center, Science 303 (2004) 1831–1838.
[11] J. Yano, J. Kern, K. Sauer, M.J. Latimer, Y. Pushkar, J. Biesiadka, B. Loll, W. Saenger, J. Messinger, A. Zouni, V.K. Yachandra, Where water is oxidized to dioxygen: structure of the photosynthetic Mn_4Ca cluster, Science 314 (2006) 821–825.
[12] B. Kok, B. Forbush, M. McGloin, Cooperation of charges in photosynthetic O_2 evolution, Photochem. Photobiol. 11 (1970) 457–476.
[13] W. Hillier, J. Messinger, Mechanism of photosynthetic oxygen production, in: T. Wydrzynski, K. Satoh (Eds.), Photosystem II. The Light-driven Water:Plastoquinone Oxidoredutase, Springer, Dordrecht, 2005, pp. 567–608.
[14] P.E.M. Siegbahn, M. Lundberg, The mechanism for dioxygen formation in PSII studied by quantum chemical methods, Photochem. Photobiol. Sci. 4 (2005) 1035–1043.
[15] H. Dau, M. Haumann, The manganese complex of photosystem II in its reaction cycle—basic framework and possible realization at the atomic level, Coord. Chem. Rev. 252 (2008) 273–295.
[16] A. Klauss, M. Haumann, H. Dau, Alternating electron and proton transfer steps in photosynthetic water oxidation, Proc. Natl. Acad. Sci. U. S. A. 109 (2012) 16035–16040.
[17] J. Messinger, G. Renger, Photosynthetic water-splitting, in: G. Renger (Ed.), Primary Processes of Photosynthesis—Part 2: Basic Principles and Apparatus, The Royal Society of Chemistry, Cambridge, UK, 2008, pp. 291–349.
[18] R.D. Britt, K.A. Campbell, J.M. Peloquin, M.L. Gilchrist, C.P. Aznar, M.M. Dicus, J. Robblee, J. Messinger, Recent pulsed EPR studies of the photosystem II oxygen-evolving complex: implications as to water oxidation mechanisms, Biochim. Biophys. Acta 1655 (2004) 158–171.
[19] T. Noguchi, FTIR detection of water reactions in the oxygen-evolving centre of photosystem II, Philos. Trans. R. Soc. Lond. B Biol. Sci. 363 (2008) 1189–1194.
[20] D. Shevela, K. Beckmann, J. Clausen, W. Junge, J. Messinger, Membrane-inlet mass spectrometry reveals a high driving force for oxygen production by photosystem II, Proc. Natl. Acad. Sci. U. S. A. 108 (2011) 3602–3607.
[21] J. Messinger, M. Badger, T. Wydrzynski, Detection of *one* slowly exchanging substrate water molecule in the S_3 state of photosystem II, Proc. Natl. Acad. Sci. U. S. A. 92 (1995) 3209–3213.
[22] W. Hillier, T. Wydrzynski, ^{18}O–water exchange in photosystem II: substrate binding and intermediates of the water splitting cycle, Coord. Chem. Rev. 252 (2008) 306–317.
[23] W. Ames, D.A. Pantazis, V. Krewald, N. Cox, J. Messinger, W. Lubitz, F. Neese, Theoretical evaluation of structural models of the S_2 state in the oxygen evolving complex of photosystem II: protonation states and magnetic interactions, J. Am. Chem. Soc. 133 (2011) 19743–19757.
[24] P.E.M. Siegbahn, Structures and energetics for O_2 formation in photosystem II, Acc. Chem. Res. 42 (2009) 1871–1880.
[25] S. Luber, I. Rivalta, Y. Umena, K. Kawakami, J.R. Shen, N. Kamiya, G.W. Brudvig, V.S. Batista, S_1-state model of the O_2-evolving complex of photosystem II, Biochemistry 50 (2011) 6308–6311.
[26] M. Kusunoki, S_1-state Mn_4Ca complex of Photosystem II exists in equilibrium between the two most-stable isomeric substates: XRD and EXAFS evidence, J. Photochem. Photobiol. B: Biol. 104 (2011) 100–110.
[27] W. Hillier, T. Wydrzynski, The affinities for the two substrate water binding sites in the O_2 evolving complex of photosystem II vary independently during S-state turnover, Biochemistry 39 (2000) 4399–4405.
[28] J. Messinger, Evaluation of different mechanistic proposals for water oxidation in photosynthesis on the basis of Mn_4O_xCa structures for the catalytic site and spectroscopic data, Phys. Chem. Chem. Phys. 6 (2004) 4764–4771.
[29] J.H. Robblee, J. Messinger, R.M. Cinco, K.L. McFarlane, C. Fernandez, S.A. Pizarro, K. Sauer, V.K. Yachandra, The Mn cluster in the S_0 state of the oxygen-evolving complex of photosystem II studied by EXAFS spectroscopy: are there three di-□-oxo-bridged Mn_2 moieties in the tetranuclear Mn complex? J. Am. Chem. Soc. 124 (2002) 7459–7471.
[30] J. Messinger, J.H. Robblee, U. Bergmann, C. Fernandez, P. Glatzel, H. Visser, R.M. Cinco, K.L. McFarlane, E. Bellacchio, S.A. Pizarro, S.P. Cramer, K. Sauer, M.P. Klein, V.K. Yachandra, Absence of Mn centered oxidation in the S_2 to S_3 transition: implications for the mechanism of photosynthetic water oxidation, J. Am. Chem. Soc. 123 (2001) 7804–7820.
[31] K. Beckmann, J. Messinger, M.R. Badger, T. Wydrzynski, W. Hillier, On-line mass spectrometry: membrane inlet sampling, Photosynth. Res. 102 (2009) 511–522.
[32] L. Konermann, J. Messinger, W. Hillier, Mass spectrometry based methods for studying kinetics and dynamics in biological systems, in: T.J. Aartsma, J. Matysik (Eds.), Biophysical Techniques in Photosynthesis, vol. II, Springer, Dordrecht, 2008, pp. 167–190.
[33] W. Hillier, T. Wydrzynski, Oxygen ligand exchange at metal sites: implications for the O_2 evolving mechanism of photosystem II, Biochim. Biophys. Acta 1503 (2001) 197–209.
[34] W. Hillier, T. Wydrzynski, Substrate water interactions within the photosystem II oxygen evolving complex, Phys. Chem. Chem. Phys. 6 (2004) 4882–4889.
[35] W. Hillier, J. Messinger, T. Wydrzynski, Kinetic determination of the fast exchanging substrate water molecule in the S_3 state of photosystem II, Biochemistry 37 (1998) 16908–16914.
[36] W. Hillier, G. Hendry, R.L. Burnap, T. Wydrzynski, Substrate water exchange in photosystem II depends on the peripheral proteins, J. Biol. Chem. 276 (2001) 46917–46924.

[37] G. Hendry, T. Wydrzynski, The two substrate water molecules are already bound to the oxygen evolving complex in the S_2 state of photosystem II, Biochemistry 41 (2002) 13328–13334.

[38] L.V. Kulik, B. Epel, W. Lubitz, J. Messinger, Electronic structure of the Mn_4O_xCa cluster in the S_0 and S_2 states of the oxygen-evolving complex of photosystem II based on pulse ^{55}Mn ENDOR and EPR Spectroscopy, J. Am. Chem. Soc. 129 (2007) 13421–13435.

[39] W. Liang, T.A. Roelofs, R.M. Cinco, A. Rompel, M.J. Latimer, W.O. Yu, K. Sauer, M.P. Klein, V.K. Yachandra, Structural change of the Mn cluster during the S_2 to S_3 state transition of the oxygen evolving complex of photosystem II. Does it reflect the onset of water/substrate oxidation? Determination by Mn X-ray absorption spectroscopy, J. Am. Chem. Soc. 122 (2000) 3399–3412.

[40] M. Haumann, C. Müller, P. Liebisch, L. Iuzzolino, J. Dittmer, M. Grabolle, T. Neisius, W. Meyer-Klaucke, H. Dau, Structural and oxidation state changes of the photosystem II manganese complex in four transitions of the water oxidation cycle ($S_0 \rightarrow S_1$, $S_1 \rightarrow S_2$, $S_2 \rightarrow S_3$, and S_3, $S_4 \rightarrow S_0$) characterized by X-ray absorption spectroscopy at 20 K and room temperature, Biochemistry 44 (2005) 1894–1908.

[41] G. Hendry, T. Wydrzynski, ^{18}O isotope exchange measurements reveal that calcium is involved in the binding of one substrate-water molecule to the oxygen-evolving complex in photosystem II, Biochemistry 42 (2003) 6209–6217.

[42] S. Singh, R.J. Debus, T. Wydrzynski, W. Hillier, Investigation of substrate water interactions at the high-affinity Mn site in the photosystem II oxygen-evolving complex, Philos. Trans. R. Soc. Lond. B Biol. Sci. 363 (2008) 1229–1234.

[43] R.J. Service, J. Yano, I. McConnell, H.J. Hwang, D. Niks, R. Hille, T. Wydrzynski, R.L. Burnap, W. Hillier, R.J. Debus, Participation of Glutamate-354 of the CP43 polypeptide in the ligation of manganese and the binding of substrate water in photosystem II, Biochemistry 50 (2011) 63–81.

[44] M. Sugiura, F. Rappaport, W. Hillier, P. Dorlet, Y. Ohno, H. Hayashi, A. Boussac, Evidence that D1-His332 in photosystem II from *Thermosynechococcus elongatus* interacts with the S_3-state and not with the S_2-state, Biochemistry 48 (2009) 7856–7866.

[45] M. Kusunoki, Mono-manganese mechanism of the photosytem II water splitting reaction by a unique Mn_4Ca cluster, Biochim. Biophys. Acta 1767 (2007) 484–492.

[46] H. Dau, C. Limberg, T. Reier, M. Risch, S. Roggan, P. Strasser, The mechanism of water oxidation: from electrolysis via homogeneous to biological catalysis, ChemCatChem 2 (2010) 724–761.

[47] E.M. Sproviero, K. Shinopoulos, J.A. Gascon, J.P. McEvoy, G.W. Brudvig, V.S. Batista, QM/MM computational studies of substrate water binding to the oxygen-evolving centre of photosystem II, Philos. Trans. R. Soc. Lond. B Biol. Sci. 363 (2008) 1149–1156.

[48] M. Lundberg, M.R.A. Blomberg, P.E.M. Siegbahn, Modeling water exchange on monomeric and dimeric Mn centers, Theor. Chem. Acc. 110 (2003) 130–143.

[49] S. Petrie, R. Stranger, R.J. Pace, Location of potential substrate water binding sites in the water oxidizing complex of photosystem II, Angew. Chem. Int. Ed. 49 (2010) 4233–4236.

[50] J.W. Murray, K. Maghlaoui, J. Kargul, N. Ishida, T.L. Lai, A.W. Rutherford, M. Sugiura, A. Boussac, J. Barber, X-ray crystallography identifies two chloride binding sites in the oxygen evolving centre of photosystem II, Energy Environ. Sci. 1 (2008) 161–166.

[51] F.M. Ho, S. Styring, Access channels and methanol binding site to the $CaMn_4$ cluster in photosystem II based on solvent accessibility simulations, with implications for substrate water access, Biochim. Biophys. Acta 1777 (2008) 140–153.

[52] J.W. Murray, J. Barber, Structural characteristics of channels and pathways in photosystem II including the identification of an oxygen channel, J. Struct. Biol. 159 (2007) 228–237.

[53] S. Vassiliev, T. Zaraiskaya, D. Bruce, Exploring the energetics of water permeation in photosystem II by multiple steered molecular dynamics simulations, Biochim. Biophys. Acta 1817 (2012) 1671–1678.

[54] P.E.M. Siegbahn, Water oxidation mechanism in photosystem II, including oxidations, proton release pathways, O – O bond formation and O_2 release, Biochim. Biophys. Acta (2012), http://dx.doi.org/10.1016/j.bbabio.2012.1010.1006.

[55] J. Yano, J. Kern, K.D. Irrgang, M.J. Latimer, U. Bergmann, P. Glatzel, Y. Pushkar, J. Biesiadka, B. Loll, K. Sauer, J. Messinger, A. Zouni, V.K. Yachandra, X-ray damage to the Mn_4Ca complex in single crystals of photosystem II: a case study for metalloprotein crystallography, Proc. Natl. Acad. Sci. U. S. A. 102 (2005) 12047–12052.

[56] A. Galstyan, A. Robertazzi, E.W. Knapp, Oxygen-evolving Mn cluster in photosystem II: the protonation pattern and oxidation state in the high-resolution crystal structure, J. Am. Chem. Soc. 134 (2012) 7442–7449.

[57] M. Grabolle, M. Haumann, C. Müller, P. Liebisch, H. Dau, Rapid loss of structural motifs in the manganese complex of oxygenic photosynthesis by X-ray irradiation at 10–300 K, J. Biol. Chem. 281 (2006) 4580–4588.

[58] P. Gatt, S. Petrie, R. Stranger, R.J. Pace, Rationalizing the 1.9 Å crystal structure of photosystem II—a remarkable Jahn–Teller balancing act induced by a single proton transfer, Angew. Chem. Int. Ed. Engl. 51 (2012) 12025–12028.

[59] D.R.J. Kolling, N. Cox, G.M. Ananyev, R.J. Pace, G.C. Dismukes, What are the oxidation states of manganese required to catalyze photosynthetic water oxidation? Biophys. J. 103 (2012) 313–322.

[60] L.V. Kulik, B. Epel, W. Lubitz, J. Messinger, ^{55}Mn pulse ENDOR at 34 GHz of the S_0 and S_2 states of the oxygen-evolving complex in photosystem II, J. Am. Chem. Soc. 127 (2005) 2392–2393.

[61] P. Glatzel, J. Yano, U. Bergmann, H. Visser, J.H. Robblee, W.W. Gu, F.M.F. de Groot, S.P. Cramer, V.K. Yachandra, Resonant inelastic X-ray scattering (RIXS) spectroscopy at the Mn K absorption pre-edge—a direct probe of the 3d orbitals, J. Phys. Chem. Solids 66 (2005) 2163–2167.

[62] P.E.M. Siegbahn, An energetic comparison of different models for the oxygen evolving complex of photosystem II, J. Am. Chem. Soc. 131 (2009) 18238–18239.

[63] S. Petrie, R. Stranger, P. Gatt, R.J. Pace, Bridge over troubled water: resolving the competing photosystem II crystal structures, Chem. Eur. J. 13 (2007) 5082–5089.

[64] T. Noguchi, M. Sugiura, FTIR detection of water reactions during the flash-induced S-state cycle of the photosynthetic water-oxidizing complex, Biochemistry 41 (2002) 15706–15712.

[65] W. Hillier, G.T. Babcock, S-state dependent Fourier transform infrared difference spectra for the photosystem II oxygen evolving complex, Biochemistry 40 (2001) 1503–1509.

[66] D.A. Pantazis, W. Ames, N. Cox, W. Lubitz, F. Neese, Two interconvertible structures that explain the spectroscopic properties of the oxygen-evolving complex of photosystem II in the S_2 state, Angew. Chem. Int. Ed. 51 (2012) 9935–9940.

[67] G. Renger, Photosynthetic water oxidation to molecular oxygen: apparatus and mechanism, Biochim. Biophys. Acta 1503 (2001) 210–228.

[68] R. Tagore, R.H. Crabtree, G.W. Brudvig, Distinct mechanisms of bridging-oxo exchange in di-μ-O dimanganese complexes with and without water-binding sites: implications for water binding in the O_2-evolving complex of photosystem II, Inorg. Chem. 46 (2007) 2193–2203.

[69] R. Tagore, H.Y. Chen, R.H. Crabtree, G.W. Brudvig, Determination of μ-oxo exchange rates in di-μ-oxo dimanganese complexes by electrospray ionization mass spectrometry, J. Am. Chem. Soc. 128 (2006) 9457–9465.

[70] A. Boussac, J.L. Zimmermann, A.W. Rutherford, J. Lavergne, Histidine oxidation in the oxygen-evolving photosystem II enzyme, Nature 347 (1990) 303–306.

[71] R. de Wijn, H.J. van Gorkom, S-state dependence of the miss probability in photosystem II, Photosynth. Res. 72 (2002) 217–222.

[72] H. Suzuki, M. Sugiura, T. Noguchi, Determination of the miss probabilities of individual S-state transitions during photosynthetic water oxidation by monitoring electron flow in photosystem II using FTIR spectroscopy, Biochemistry 51 (2012) 6776–6785.

[73] S. Isgandarova, G. Renger, J. Messinger, Functional differences of photosystem II from *Synechococcus elongatus* and spinach characterized by flash induced oxygen evolution patterns, Biochemistry 42 (2003) 8929–8938.

[74] G.Y. Han, F. Mamedov, S. Styring, Misses during water oxidation in photosystem II are S state-dependent, J. Biol. Chem. 287 (2012) 13422–13429.

[75] S. Yamanaka, H. Isobe, K. Kanda, T. Saito, Y. Umena, K. Kawakami, J.R. Shen, N. Kamiya, M. Okumura, H. Nakamura, K. Yamaguchi, Possible mechanisms for the O – O bond formation in oxygen evolution reaction at the $CaMn_4O_5(H_2O)_4$ cluster of PSII refined to 1.9 Å X-ray resolution, Chem. Phys. Lett. 511 (2011) 138–145.

[76] E.M. Sproviero, J.A. Gascon, J.P. McEvoy, G.W. Brudvig, V.S. Batista, Quantum mechanics/molecular mechanics study of the catalytic cycle of water splitting in photosystem II, J. Am. Chem. Soc. 130 (2008) 3428–3442.

[77] L. Rapatskiy, N. Cox, A. Savitsky, W.M. Ames, J. Sander, M.M. Nowaczyk, M. Rogner, A. Boussac, F. Neese, J. Messinger, W. Lubitz, Detection of the water-binding sites of the oxygen-evolving complex of photosystem II using W-band ^{17}O Electron–Electron Double Resonance-detected NMR spectroscopy, J. Am. Chem. Soc. 134 (2012) 16619–16634.

[78] T. Saito, S. Yamanaka, K. Kanda, H. Isobe, Y. Takano, Y. Shigeta, Y. Umena, K. Kawakami, J.R. Shen, N. Kamiya, M. Okumura, M. Shoji, Y. Yoshioka, K. Yamaguchi, Possible mechanisms of water splitting reaction based on proton and electron release pathways revealed for $CaMn_4O_5$ cluster of PSII refined to 1.9 Å X-ray resolution, Int. J. Quantum Chem. 112 (2012) 253–276.

[79] Y.L. Pushkar, J. Yano, K. Sauer, A. Boussac, V.K. Yachandra, Structural changes in the Mn_4Ca cluster and the mechanism of photosynthetic water splitting, Proc. Natl. Acad. Sci. U. S. A. 105 (2008) 1879–1884.

[80] O.M. Usov, V.M. Grigoryants, R. Tagore, G.W. Brudvig, C.P. Scholes, Hyperfine coupling to the bridging ^{17}O in the di-μ-oxo core of a Mn^{III}–Mn^{IV} model significant to the core electronic structure of the O_2-evolving complex in photosystem II, J. Am. Chem. Soc. 129 (2007) 11886–11887.

[81] I.L. McConnell, V.M. Grigoryants, C.P. Scholes, W.K. Myers, P.Y. Chen, J.W. Whittaker, G.W. Brudvig, EPR-ENDOR characterization of ^{17}O, ^{1}H, ^{2}H water in manganese catalase and its relevance to the oxygen-evolving complex of photosystem II, J. Am. Chem. Soc. 134 (2012) 1504–1512.

[82] P.E.M. Siegbahn, A structure consistent mechanism for dioxygen formation in photosystem II, Chem. Eur. J. 14 (2008) 8290–8302.

[83] P.E.M. Siegbahn, O – O bond formation in the S_4 state of the oxygen-evolving complex in photosystem II, Chem. Eur. J. 12 (2006) 9217–9227.

[84] G. Renger, Mechanism of light induced water splitting in photosystem II of oxygen evolving photosynthetic organisms, Biochim. Biophys. Acta 1817 (2012) 1164–1176.

[85] P. Geijer, F. Morvaridi, S. Styring, The S_3 state of the oxygen evolving complex in photosystem II is converted to the $S_2Y_Z^{\bullet}$ state at alkaline pH, Biochemistry 40 (2001) 10881–10891.

[86] H. Suzuki, M. Sugiura, T. Noguchi, Monitoring water reactions during the S-state cycle of the photosynthetic water-oxidizing center: detection of the DOD bending vibrations by means of Fourier transform infrared spectroscopy, Biochemistry 47 (2008) 11024–11030.

[87] M.A. Strickler, H.J. Hwang, R.L. Burnap, J. Yano, L.M. Walker, R.J. Service, R.D. Britt, W. Hillier, R.J. Debus, Glutamate-354 of the CP43 polypeptide interacts with the oxygen-evolving Mn_4Ca cluster of photosystem II: a preliminary

characterization of the Glu354Gln mutant, Philos. Trans. R. Soc. Lond. B Biol. Sci. 363 (2008) 1179–1187.
[88] W. Hillier, I. McConnell, S. Singh, R. Debus, A. Boussac, T. Wydrzynski, Substrate water exchange in photosystem II: insights from mutants and Ca vs. Sr substitution, in: J.F. Allen, E. Gantt, J.H. Golbeck, B. Osmond (Eds.), Photosynthesis. Energy from the Sun, Springer, Dordrecht, 2008, pp. 427–430.
[89] H. Ishikita, W. Saenger, B. Loll, J. Biesiadka, E.W. Knapp, Energetics of a possible proton exit pathway for water oxidation in photosystem II, Biochemistry 45 (2006) 2063–2071.
[90] P.E.M. Siegbahn, M. Lundberg, Hydroxide instead of bicarbonate in the structure of the oxygen evolving complex, J. Inorg. Biochem. 100 (2006) 1035–1040.
[91] Y. Shimada, H. Suzuki, T. Tsuchiya, T. Tomo, T. Noguchi, M. Mimuro, Effect of a single-amino acid substitution of the 43 kDa chlorophyll protein on the oxygen-evolving reaction of the cyanobacterium *Synechocystis* sp PCC 6803: analysis of the Glu354Gln Mutation, Biochemistry 48 (2009) 6095–6103.
[92] M.A. Strickler, L.M. Walker, W. Hillier, R.D. Britt, R.J. Debus, No evidence from FTIR difference spectroscopy that aspartate-342 of the D1 polypeptide ligates a Mn ion that undergoes oxidation during the S-0 to S-1, S-1 to S-2, or S-2 to S-3 transitions in photosystem II, Biochemistry 46 (2007) 3151–3160.
[93] R.J. Debus, Protein ligation of the photosynthetic oxygen-evolving center, Coord. Chem. Rev. 252 (2008) 244–258.
[94] J.P. McEvoy, G.W. Brudvig, Structure-based mechanism of photosynthetic water oxidation, Phys. Chem. Chem. Phys. 6 (2004) 4754–4763.
[95] J. Yano, V.K. Yachandra, Where water is oxidized to dioxygen: structure of the photosynthetic Mn_4Ca cluster from X-ray spectroscopy, Inorg. Chem. 47 (2008) 1711–1726.
[96] J. Yano, J. Kern, Y. Pushkar, K. Sauer, P. Glatzel, U. Bergmann, J. Messinger, A. Zouni, V.K. Yachandra, High-resolution structure of the photosynthetic Mn_4Ca catalyst from X-ray spectroscopy, Philos. Trans. R. Soc. Lond. B Biol. Sci. 363 (2008) 1139–1147.
[97] Y. Pushkar, J. Yano, P. Glatzel, J. Messinger, A. Lewis, K. Sauer, U. Bergmann, V. Yachandra, Structure and orientation of the Mn4Ca cluster in plant photosystem II membranes studied by polarized range-extended X-ray absorption spectroscopy, J. Biol. Chem. 282 (2007) 7198–7208.
[98] H. Dau, A. Grundmeier, P. Loja, M. Haumann, On the structure of the manganese complex of photosystem II: extended-range EXAFS data and specific atomic-resolution models for four S-states, Philos. Trans. R. Soc. Lond. B Biol. Sci. 363 (2008) 1237–1243.
[99] H. Dau, P. Liebisch, M. Haumann, The structure of the manganese complex of Photosystem II in its dark-stable S_1-state—EXAFS results in relation to recent crystallographic data, Phys. Chem. Chem. Phys. 6 (2004) 4781–4792.
[100] F. Rappaport, M. Blanchard-Desce, J. Lavergne, Kinetics of electron transfer and electrochromic change during the redox transitions of the photosynthetic oxygen evolving complex, Biochim. Biophys. Acta 1184 (1994) 178–192.
[101] F. Rappaport, N. Ishida, M. Sugiura, A. Boussac, Ca^{2+} determines the entropy changes associated with the formation of transition states during water oxidation by Photosystem II, Energy Environ. Sci. 4 (2011) 2520–2524.
[102] M. Haumann, P. Liebisch, C. Müller, M. Barra, M. Grabolle, H. Dau, Photosynthetic O_2 formation tracked by time-resolved X-ray experiments, Science 310 (2005) 1019–1021.
[103] L. Gerencser, H. Dau, Water oxidation by photosystem II: H_2O–D_2O exchange and the influence of pH support formation of an intermediate by removal of a proton before dioxygen creation, Biochemistry 49 (2010) 10098–10106.
[104] M.R. Razeghifard, R.J. Pace, EPR kinetic studies of oxygen release in thylakoids in PSII membranes: a kinetic intermediate in the S_3 to S_0 transition, Biochemistry 38 (1999) 1252–1257.
[105] T. Noguchi, H. Suzuki, M. Tsuno, M. Sugiura, C. Kato, Time-resolved infrared detection of the proton and protein dynamics during photosynthetic oxygen evolution, Biochemistry 51 (2012) 3205–3214.